

A novel electronic subdivision method of automatic interference comparator

CHANG Haitao¹, YE Xiaoyou², GAO Hongtang² and WANG Zhongyu^{1, #}

¹ School of Instrumentation Science & Opto-Electronics Engineering, Beihang University, No.37 Xue Yuan Lu, Beijing, China, 100191

² Division of Metrology in Length and Precision Engineering, NIM, No.18 Bei San Huan Dong Lu, Beijing, China, 100013

Corresponding Author / E-mail: mewan@buaa.edu.cn, TEL: +86-010-82338881, FAX: +86-010-82338881

KEYWORDS : Length measurement, Calibration, Subdivision, Fringe counting

Automatic interference comparator (AIC) is a high precision one-dimensional length measurement machine for investigation and calibrations of line scales, linear encoders and length gauges. This paper emphasizes a novel electronic subdivision method for the AIC to realize precision measurement, which is composed of integer fringe counting, fraction fringe counting and electronic strobe. The realization of the whole system is based on FPGA. A standard line scale has been calibrated on the National Institute of Metrology of China (NIM)'s AIC with this method. The experimental results show the measurement repeatability less than 7.5 nm, which demonstrate the feasibility of the signal processing method.

Manuscript received: January XX, 2011 / Accepted: January XX, 2011

1. Introduction

All kinds of accurate measurements are vitally important to many scientific and industrial operations, and measurement of length is fundamental^[1]. Since Michelson first proposed the use of interferometers for the measurement of length in 1887, optical interferometry measurements have become essential as metrology thanks to their higher accuracy^[2]. In 1983, the General Conference of Weights & Measures defined the meter as the path length traveled by light in vacuum in 1/299792458 second. Along with the 1983 action, the CGPM sanctioned iodine stabilized helium neon lasers as working length standards for relatively short lengths^[3].

A sufficiently accurate method for fringe subdivision must be used, when nanometer resolution is required. There are two useful methods of subdivision. One is optical subdivision, and the other is electronic fringe subdivision. The optical subdivision utilizes an appropriate optical configuration design or features of optical elements to multiple optical path difference to subdivide the fringe. Optical subdivision is the most efficient method, unfortunately it can only achieve a lesser extent because of the limit of the optical systems, commonly it is 1/4 wavelength, while 1/16 wavelength is rare^[4, 5]. Due to restrictions on the number of subdivision, high precision length measurement mainly uses electrical techniques to subdivide interference fringes. By use of a fast analog-to-digital converter and integrated digital circuits, the electronic subdivision factors of 1/100 ~ 1/2000 can be obtained.

In this paper, a novel electronic subdivision based on Coordinate

Rotation Digital Computer (CORDIC) algorithm is proposed. Two orthogonal interference signals are electrically divided into thousands by the signal processing circuit implemented on FPGA^[6, 7]. With this circuit, spurious triggers caused by possible defects, such as scratches, corrosion, dirty spots, etc., on the measuring surface of the scale can be eliminated. A new integer fringe counting method according to the displacement corresponding to the fraction number is described. The integer fringe counting error can be avoided by this method. Its feasibility was also verified by experiment on NIM² AIC.

2. Principle of interference measuring

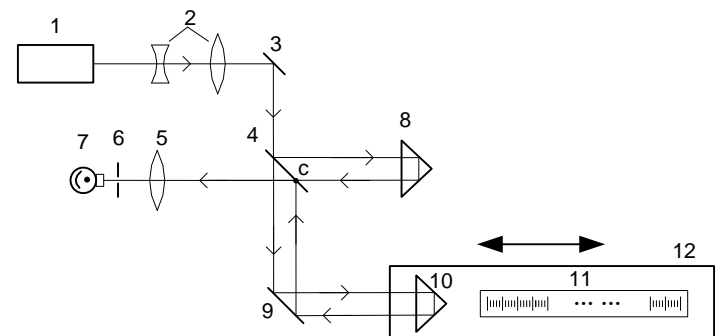


Fig. 1 Length measuring interferometer

1 laser, 2 collimation lens, 3 mirror, 4 beam splitter, 5 lens, 6 pinhole, 7 photo-detector, 8 fixed mirror, 9 mirror, 10 moving mirror, 11 scale, 12 measurement carriage.

The set-up of the AIC is shown in Fig. 1. This is a classical

Michelson interferometer with one moving mirror 10 on the measurement carriage 12 and a fixed mirror 8. The light is emitted by frequency stabilized He-Ne laser 1. Through the collimation lens 2, the light is divided by a beam splitter 4 oriented at 45 degrees to the beam. One beam travels to the fixed mirror 8, where it is back reflected to beam splitter 4. The other beam travels to the moving mirror 10 where it is reflected. Both reflected beams recombine at point C on the splitter 4 to produce interference fringes (assuming proper alignment). Through the pinhole 6, the fringes are detected by photo-detector 7. Precise distance measurements can be made with the Michelson interferometer by moving the measurement carriage and counting the interference fringes^[8, 9].

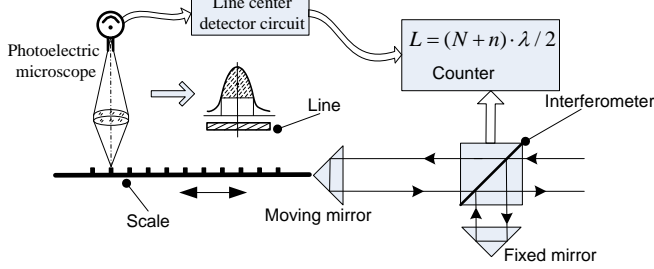


Fig. 2 Principle diagram of interference measuring

Line scales are calibrated by making carriage displacement. The principle diagram of interference measuring is shown in Fig. 2. When the line appears in the microscope field, the image of line will be received and converted into electrical signal by photoelectric microscope^[10, 11]. The shape of the electrical signal is shown in Fig. 2, corresponding exactly to the line width. A line center detector circuit can give the coordinates of the middle of the line^[12]. According to the coordinates, we obtain the integer fringes number N and fraction number n . The distance L , can be calculated by

$$L = (N + n) \cdot \lambda / 2 \quad (1)$$

Where, N is the integer number of fringes; n is the fraction number of the fringes; λ is the wavelength, one interference fringe corresponds to a distance or a length of $\lambda/2$.

For example, by using a light source of $\lambda = 532\text{nm}$, the basic 'unit' of measurement is 266 nm in size of one fringe. Hence value of N alone provides a measurement resolution of 266 nm. By careful analyzing these interference fringes, it is possible to sub-divide them (and hence measure n) to a resolution of 1/100 to 1/1000 of a fringe, nanometer resolution can be achieved.

3. Interference signal processing

The interference signals processing is the key part of the AIC, which is composed of integer fringe counting, fraction fringe counting and electronic strobe. At present, the optical fringe counting methods are divided into hardware and software fringe counting. The hardware fringe counting method, which is easy to realize and has the advantage of good real-time performance has become more generally preferred.

3.1 Fraction fringe counting

The interference signals obtained by the photo-detectors are converted into two orthogonal signals. Generally speaking, the two signals are assumed to have 90 degrees difference, and their

amplitude as well as DC offset should be same. Therefore, they can be represented cosine and sinusoidal signal as shown in Fig. 3. If the point C is the location of line center, the length L between the zero graduation and current graduation is calculated by Equation 1. The aim of the fraction fringe counting is to get the accurate value of n . With the high-speed data acquisition circuit, the voltages of sine and cosine can be acquired. As shown in Fig. 3, the signal CLK represents the sampling pulse of the acquisition circuit. The fraction number n is given by

$$n = \frac{\theta}{360} = \frac{\arctan \frac{U_{\sin}}{U_{\cos}}}{360} \quad (2)$$

Where, U_{\sin} is voltage of sine and U_{\cos} is the voltage of cosine. Equation 2 shows that arctangent calculation can be used to get the fraction number n . In this paper, the calculation implemented on FPGA is based on the CORDIC algorithm.

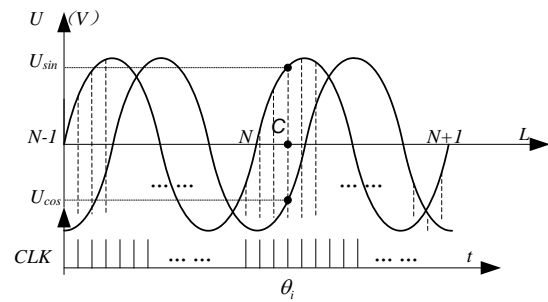


Fig. 3 Acquisition of the interference signals

The CORDIC algorithm was originally developed by Volder^[13] to iteratively solve trigonometric equations in 1959, and later generalized by Walther^[14] to solve a broader range of equations, including the discrete cosine^[15], discrete Fourier^[15] and singular value decomposition^[16,17].

All the trigonometric functions can be computed or derived from functions using vector rotations, as will be discussed in the following sections. The CORDIC algorithm provides an iterative method of performing vector rotation by arbitrary angles using only additions, subtractions and shift operations, which are convenient to implement in VHDL on FPGA.

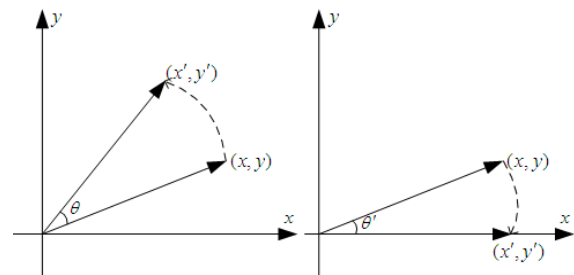


Fig. 4 Vector rotation

As shown in Fig. 4, the vector (x, y) is rotated through the angle θ yielding a new vector (x', y') , which is given by

$$x' = x \cos \theta - y \sin \theta = \cos \theta (x - y \tan \theta) \quad (3)$$

$$y' = y \cos \theta + x \sin \theta = \cos \theta (y + x \tan \theta) \quad (4)$$

With iterative method, the vector rotation is performed as a sequence of successively smaller rotations, and each of rotation angle is restricted so that arctangent (2^{-i}) . The iterative rotation can now be expressed as:

$$x' = \prod_{i=1}^n K_i (x_i - \alpha_i \cdot y_i \cdot 2^{-i}) \quad (5)$$

$$y' = \prod_{i=1}^n K_i (y_i + \alpha_i \cdot x_i \cdot 2^{-i}) \quad (6)$$

$$\theta' = \sum_{i=1}^n \alpha_i \cdot \arctan 2^{-i} \quad (7)$$

$$K_i = \cos(\arctan 2^{-i}) = 1/\sqrt{1+2^{-2i}} \quad (8)$$

Where $x_{i+1} = x_i - \alpha_i \cdot y_i \cdot 2^{-i}$; $y_{i+1} = y_i + \alpha_i \cdot x_i \cdot 2^{-i}$, $\theta_{i+1} = \theta_i + \alpha_i \cdot \arctan 2^{-i}$, $\alpha_i = \pm 1$, when $y_{i-1} \geq 0$, α_i is set to -1 and when $y_{i-1} < 0$, α_i is set to +1. In practical application, the CORDIC algorithms are used to compute the rotation angle. The value of y' converges to zero. The iterative rotation can be expressed as:

$$x' = K_i \sqrt{x^2 + y^2} \quad (9)$$

$$y' = 0 \quad (10)$$

$$\theta' = \arctan(x/y) \quad (11)$$

Since digital signal processing technology has achieved great development, especially the appearances of high speed processors such as FPGA and DSP, fraction fringe counting based on CORDIC algorithm is implemented conveniently.

3.2 Integer fringe counting

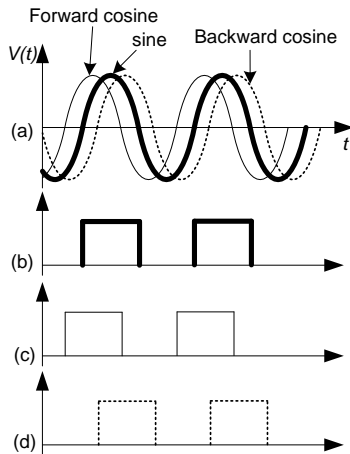


Fig. 5 Traditional integer fringe counting method

Traditional integer fringe counting method is shown in Fig. 5. In Fig. 5(a), the thick line represents the sine signal, and the thin line and the dashed line represent the cosine signal when the measured object is moving forward and backward, respectively. According to the principle of zero-cross-over triggering, the two phase-quadrature interference signals (sine and cosine) obtained by the photo-detectors are converted into square waves which are shown in Fig. 5(b), (c) and (d). The number of sine square waves is counted by a bi-directional counter.

Traditional integer fringe counting method is easy to realize, but it is prone to count incorrectly. For example, there may be some trembling of the signals at zero point (shown in Fig. 6), which caused by interference from a nearby circuit or system. In Fig. 6(b), the curve signifies arctangent values between 0 and 2π . As shown in Fig. 6(a), the angle changes three times, so the integer fringe number will be miscounted as three. However, the real displacement corresponds to

one integer number.

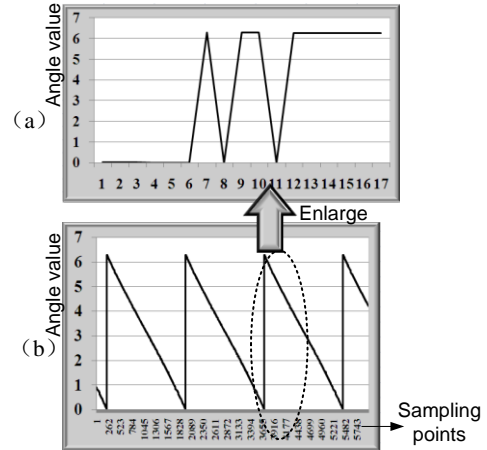


Fig. 6 Trembling at zero point

To eliminate the integer fringe counting error, we adopt a new integer fringe counting method corresponding to the fraction number. The integer fringe number has been obtained by comparing the change of arctangent values. If the angle changes from 0 to 2π , the N adds 1. Otherwise, if the angle changes from 2π to 0, N subtracts 1. An integer fringe counting module composed of a comparator and a reversible counter has been designed with VHDL language on a FPGA platform. The module is verified by experiment. Arctangent values and integer fringe number N are compared. It can be seen from Fig. 7, with the change of angle, N adds 1 or subtracts 1 automatically [18].

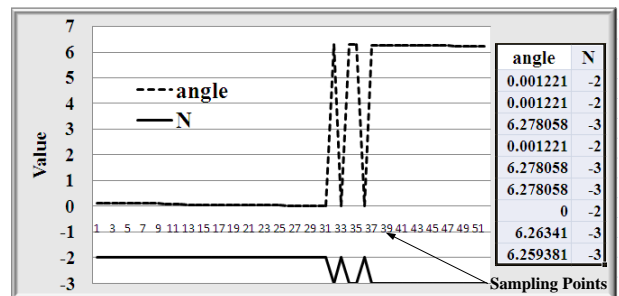


Fig. 7 Comparison of integer number and arctangent values

3.3 Electronic strobe

A scale with clear graduations is relatively easy to process. Unfortunately we also calibrate medium quality printed scales. These often present problems due to scratches or marks on the scale which cause extra triggers [19]. Trigger signals are shown in Fig. 8 traced by an oscilloscope. The scratch signal and corresponding trigger signal are boxed off. Others are line scale signals.

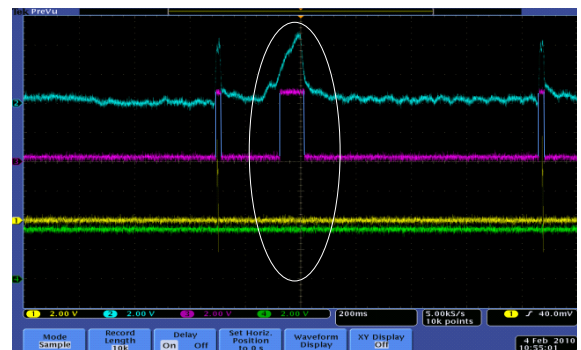


Fig. 8 Trigger signals

These extra triggers quickly lead a simple system into confusion. In this paper, an electronic strobe based on the integer fringe counting is proposed and it can effectively filtrate the extra triggers in the length measurement. Software has been developed on a FPGA platform to analyze the trigger sequence and determine the triggers correspond to the correct edges of the graduations [20]. The principle diagram has been presented in Fig. 9. There is a counter for recording the numbers of integer fringes between the two graduations. Base on the distance between the graduations, we set a proper threshold value in comparator. If the counter number is greater than the threshold value, the switch is opened, waiting for the useful trigger to process. When the process is completed, the counter is cleared, and the above operations are repeated. With this method, any other triggers occurring within the graduation must be ignored.

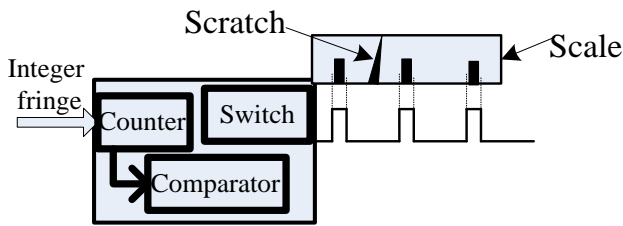


Fig. 9 Principle diagram of the electronic strobe

4. Experiment and results

4.1 Control software

Building upon National Instrument’s Lab Windows/CVI development platform, the paper established the managing software of the signal processing system for the AIC. It can control a kind of high speed PCI-I/O-card, and process the acquired data. It can also calculate the length between the two graduations of the scale and show it on the human interface. As shown in Fig. 10, the interface includes displaying of current waveforms, recording the data, and some controlling buttons. Environment parameters such as temperature, barometric pressure, air moisture content and CO₂ content are monitored and shown on the interface.

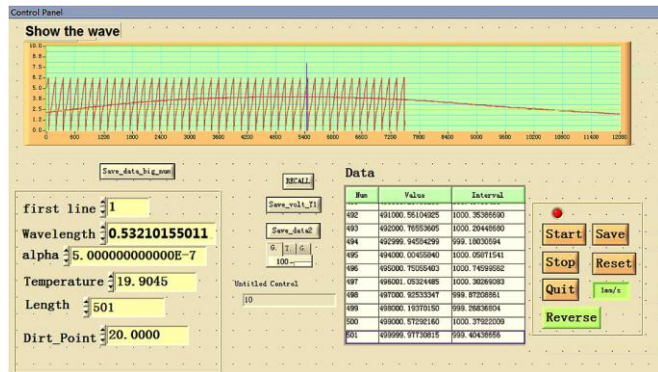


Fig. 10 Software interface

4.2 Experiment

A 200mm standard line scale has been calibrated on the NIM’s AIC with this signal processing system as shown in Fig. 11. The AIC consists of a photoelectric microscope, a high precision one-axis motion system, and a high accuracy interferometer of the Michelson type. The wavelength of the frequency-stabilized He-Ne laser corrected for temperature, humidity, atmospheric pressure, and carbon

dioxide content is used as the length standard. The instrument is housed in an environmental chamber in which all environmental properties are carefully monitored.



Fig. 11 Photo of AIC

4.2.1 Comparison measurement

Starting at the zero graduation, and ending at the terminal graduation, the interferometer measures the distances from one line center to another line center of pre-selected intervals, thus calibrating the scale. There are 201 graduations on a 200mm scale with a 1mm interval scale. Fig. 12 shows the comparison of the experiment results obtained by this AIC and 1m AIC. The 1m AIC was built by NIM to calibrate precision length standards 20 years ago, which is possible to achieve measurement uncertainty of approx 200nm for 1m. As shown in Fig.12, the abscissa is graduation of the scale, and on the ordinate the differences between the measured deviations are represented. The values of the differences are less than 200nm, which are within the uncertainty of measurement stated for the two comparators.

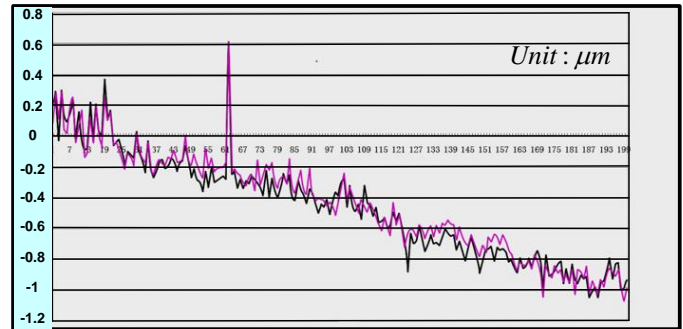


Fig. 12 Measurement data between the two instruments compared

4.2.2 Calculation of repeatability error

To calculate the repeatability error, we measured the length of the 20-foot lines which are at the foreside of the 200mm glass by repeating 14 times. Measurement data are listed in Tab. 1.

According to the National Metrological Verification of China [21], the value of the repeatability error is less than 15nm by the below equation.

$$S = \sqrt{\frac{\sum_{i=1}^{10} [vv]_i}{K(n-1)}} \quad (12)$$

Where, K is the number of intervals, here $K=10$; n is the times of the measurement, here $n=14$; $[vv]_i$ is each sum of squared residuals from 1st interval to 10th interval.

		Times													
		1	2	3	4	5	6	7	8	9	10	11	12	13	14
Graduations	1	0	0	0	0	0	0	0	0	0	0	0	0	0	0
	2	1000.112	1000.108	1000.106	1000.095	1000.119	1000.111	1000.126	1000.111	1000.116	1000.113	1000.095	1000.144	1000.116	1000.112
	3	2000.199	2000.202	2000.217	2000.205	2000.237	2000.195	2000.234	2000.208	2000.22	2000.241	2000.207	2000.219	2000.207	2000.227
	4	3000.06	3000.05	3000.037	3000.033	3000.072	3000.045	3000.059	3000.028	3000.088	3000.035	3000.051	3000.06	3000.043	3000.056
	5	4000.306	4000.295	4000.282	4000.259	4000.285	4000.29	4000.314	4000.278	4000.312	4000.267	4000.304	4000.298	4000.273	4000.299
	6	5000.113	5000.085	5000.068	5000.092	5000.105	5000.112	5000.112	5000.091	5000.106	5000.105	5000.113	5000.105	5000.099	5000.127
	7	6000.063	6000.062	6000.032	6000.025	6000.057	6000.049	6000.075	6000.032	6000.056	6000.046	6000.076	6000.084	6000.026	6000.085
	8	7000.188	7000.171	7000.191	7000.16	7000.195	7000.212	7000.19	7000.175	7000.21	7000.174	7000.211	7000.197	7000.179	7000.202
	9	8000.284	8000.311	8000.299	8000.31	8000.318	8000.318	8000.334	8000.296	8000.327	8000.333	8000.326	8000.317	8000.279	8000.323
	10	9000.03	9000.026	9000.041	9000.039	9000.055	9000.041	9000.037	9000.029	9000.039	9000.031	9000.029	9000.048	9000.038	9000.046
	11	10000.14	10000.17	10000.15	10000.15	10000.15	10000.16	10000.15	10000.16	10000.18	10000.16	10000.19	10000.18	10000.15	10000.16
	12	11000.25	11000.24	11000.25	11000.25	11000.26	11000.26	11000.25	10995.87	11000.28	11000.26	11000.28	11000.27	11000.24	11000.28
	13	12000.01	11999.95	11999.98	11999.98	11999.99	12000	12000.01	12000.02	12000.01	11999.99	11999.98	12000.01	11999.99	11999.98
	14	13000	13000.01	13000.01	12999.98	13000	13000.01	13000.01	13000.08	13000.02	13000.02	13000.02	13000.05	12999.99	13000.02
	15	14000.18	14000.19	14000.2	14000.19	14000.2	14000.23	14000.21	14000.22	14000.23	14000.19	14000.22	14000.23	14000.19	14000.22
	16	15000.07	15000.07	15000.08	15000.06	15000.06	15000.09	15000.08	15000.04	15000.09	15000.08	15000.1	15000.1	15000.07	15000.08
	17	16000.28	16000.28	16000.26	16000.25	16000.27	16000.28	16000.29	16000.3	16000.29	16000.3	16000.28	16000.3	16000.26	16000.26
	18	17000.15	17000.17	17000.16	17000.16	17000.19	17000.2	17000.2	17000.2	17000.22	17000.2	17000.21	17000.19	17000.18	17000.19
	19	18000.09	18000.08	18000.08	18000.07	18000.11	18000.13	18000.13	18000.11	18000.14	18000.12	18000.14	18000.12	18000.1	18000.12
	20	19000.43	19000.42	19000.42	19000.42	19000.45	19000.46	19000.44	19000.49	19000.47	19000.46	19000.47	19000.46	19000.43	19000.45

Table. 1 Measurement data

Times	0-1	2-3	4-5	6-7	8-9	10-11	12-13	14-15	16-17	18-19
1	0.2639	0.3121	0.3434	0.3375	0.4664	0.4194	0.4909	0.0230	-0.0421	0.3343
2	0.2607	0.3197	0.3541	0.3447	0.4673	0.4315	0.4834	0.0332	-0.0449	0.3330
3	0.2730	0.3126	0.3541	0.3518	0.4636	0.4195	0.4842	0.0237	-0.0422	0.3333
4	0.2692	0.3127	0.3466	0.3400	0.4736	0.4280	0.4886	0.0277	-0.0412	0.3353
5	0.2721	0.3183	0.3447	0.3471	0.4589	0.4422	0.4985	0.0304	-0.0412	0.3305
6	0.2570	0.3277	0.3450	0.3315	0.4720	0.4441	0.4950	0.0127	-0.0393	0.3321
7	0.2843	0.3153	0.3522	0.3390	0.4702	0.4381	0.4927	0.0173	-0.0468	0.3328
8	0.2685	0.3202	0.3617	0.3551	0.4635	0.4334	0.4735	0.0381	-0.0336	0.3396
9	0.2749	0.3221	0.3454	0.3624	0.4759	0.4296	0.4916	0.0228	-0.0269	0.3415
10	0.2652	0.3011	0.3456	0.3409	0.4759	0.4261	0.4824	0.0239	-0.0327	0.3428
11	0.2618	0.3167	0.3551	0.3517	0.4673	0.4299	0.4655	0.0162	-0.0501	0.3409
12	0.2626	0.3164	0.3534	0.3532	0.4626	0.4372	0.4749	0.0287	-0.0497	0.3353
13	0.2588	0.3060	0.3513	0.3381	0.4560	0.4343	0.4908	0.0183	-0.0506	0.3276
14	0.2664	0.3088	0.3385	0.3469	0.4546	0.4069	0.4924	0.0256	-0.0346	0.3498

Table. 2 Measurement data with new method

We usually require two interference signals with the phase difference of approximately 90^0 for bi-directional counting and fringe subdivision. Although there is dedicated circuit to collect two phase-quadrature signals, and calculate the DC offsets, the AC amplitudes and the difference from the phase-quadrature by the elliptical fitting with a least square method^[22], error still exists.

In interferometry, the two interference signals (sine and cosine) are used to determine the direction of the carriage movement. Due to mechanical reasons, sometimes rail movement may not be smooth, there will be jitter. At this point, the integer fringe counter will add 1 or subtract 1 according to the direction signal. If we can ensure that the movement of the measurement carriage is smooth and single direction, fringe subdivision can be achieved with only one interference signal (sine).

From the above discussion, another experiment has been done. Synthetic cosine signal based on sine has been built. In this method, we can assure that the two signals (sine and cosine) have 90 degrees difference, and their amplitude as well as DC offset is the same. Deviation of the data has been shown in Tab. 2. Following Equation 12, the value of the repeatability error is obtained less than 7.5nm.

5. Conclusions

The interference signal processing system for the AIC has been discussed in detail to realize precision measurement. A fraction fringe counting method based on CORDIC algorithm is proposed. A new integer fringe counting method corresponding to the fraction number is described. A standard line scale has been calibrated on the AIC with this signal processing system and the measurement repeatability is less than 7.5 nm. The system can also automatically identify the scratches or marks on the scale.

ACKNOWLEDGEMENT

This project was supported by the science foundation of NIM (Grants No. SJG0301 and AKT0733).

REFERENCES

1. Bosse, H., Koenders, L., Hatrig, F., Buhr, E. and Wilkening, G., "Nano- and Micrometrology at PTB: State of the Art and Future Challenges," *Optoelectronics, instrumentation, and data processing*, Vol. 46, No. 4, pp. 312-317, 2010.
2. Peggs, G. N. and Yacoot, A., "A Review of Recent Work in Sub-nanometer Displacement Measurement using Optical and X-ray interferometry," *Phil. Trans. R. Soc. Lond. A*, Vol. 360, No. 1794, pp. 953-968, 2002.
3. Hyun, S. W., Kim, Y. J., Kim, Y.S., Jin, J.H. and Kim, H. W., "Absolute Length Measurement with the Frequency Comb of a Femtosecond laser," *Meas. Sci. Technol.*, Vol. 20, No.19, pp. 1-6, 2009.
4. Birch, K. P., "Optical Fringe Subdivision with Nanometric accuracy," *Precision Eng.*, Vol. 12, No.4, pp. 195-198, 1990.
5. ZHANG, Z. P., CHENG Z. G., QIN Z. Y., ZHU J. Q., "A Novel Optical Subdivision Method for Dual-frequency Interferometer", *Optik- International Journal for Light and Electron Optics*, Vol. 119, No.16, pp. 772-776, 2008.
6. Valls, J., "Evaluation of CORDIC Algorithms for FPGA Design," *Journal of VLSI Signal Processing*, Vol. 32, No. 3, pp. 207-222, 2002.
7. Fons, F., Fons, M. and Lopez, M., "Trigonometric Computing Embedded in a Dynamically Reconfigurable CORDIC System-on-Chip," *Reconfigurable computing: Architectures and applications*, Vol. 3985, pp. 122-127, 2006.
8. Sawabe, M., Maeda F., et al., "A New Vacuum Interferometric Comparator for Calibrating the Fine Linear Encoders and Scales," *Precision Engineering*, Vol. 28, No.3, pp. 320-328, 2004.
9. Howick, E. F. and Sutton, C. M., "Development of an Automatic Line Scale Measuring Instrument," *Proc. SPIE*, Vol. 4401, pp. 112-119, 2001.
10. Flugge, J. and Weichert, Ch., "Interferometry at the PTB Nanometer Comparator – Design, Status and Development," *SPIE--The International Society for Optical Engineering*, Vol. 7133, pp. 713346.7-713346.8, 2008.
11. Beers, J. S., and Penzes, W. B., "The NIST Length Scale Interferometer," *Journal of Research of the National Institute of Standards and Technology*, Vol. 104, No. 3, pp. 225-252, 1999.
12. Kimura, A., GAO, W., Arai, Y. and LI, J. Z., "Design and construction of a two-degree-of-freedom linear encoder for nanometric measurement of stage position and straightness," *Precision Engineering*, Vol. 34, No. 1, pp. 145-155, 2010.
13. Volder, J., "The CORDIC Trigonometric Computing Technique," *IRE Transactions on Electronic Computers*, Vol. 8, pp. 330-334, 1959.
14. Walther, J. S., "A Unified Algorithm for Elementary Functions," *Spring Joint Computer conference*, pp. 379-385, 1971.
15. Phatak, D. S., "Double Step Branching CORDIC: A New Algorithm for Fast Sine and Cosine Generation," *IEEE Transactions on computers*, Vol. 47, No. 5, pp. 587-602, 1998.
16. Sibul L. H. and Fogelsanger A. L., "Application of Coordinate Rotation Algorithm to Singular Value Decomposition," *IEEE Int. Symp. Circuits and Systems*, pp. 821-824, 1984.
17. Valls. J and et al., "The Use of CORDIC in Software Defined Radios: A Tutorial," *IEEE Communications. Magazine*, Vol. 44, No. 9, pp. 46-50, 2006.
18. Eom, T. B. and Han, J. W. "A Precision Length Measuring System for A Variety of Linear Artefacts," *Meas. Sci. Technol.*, Vol. 12, No. 6, pp. 698-701, 2002.
19. Fedorin, V. L. and Khavinson, L. F., "Dynamic Measurement of the Length of Line Gauges," *Measurement Techniques*, Vol. 38, No. 8, pp. 873-875, 1995.
20. Jens Flügge, Rainer Köning, "Status of the Nanometer Comparator at PTB," *Proc. SPIE*, Vol. 4401, pp. 275-283, 2001.
21. JJG 331- 1994, National Metrological Verification of China, 1994.
22. Eom, T. B. and Kim, J. Y., "The Dynamic Compensation of Nonlinearity in a Homodyne Laser Interferometer," *Meas. Sci. and Technol.*, Vol.12, pp. 1-5, 2001.